Application of Visible-Near Infrared and Short Wave Infrared Spectroscopy to Sediment-hosted Zn-Pb Deposit Exploration in the Selwyn Basin, Yukon

J.M. Peter
Central Canada Division, Geological Survey of Canada, 601 Booth Street, Ottawa, ON, K1A 0E8

D. Layton-Matthews, M.G. Gadd, S. Gill, S. Baker, S. Plett
Department of Geological Sciences and Geological Engineering, Queen's University, Kingston, ON, K7L 3N6

S. Paradis
Pacific Division, Geological Survey of Canada, 9860 West Saanich Road, Sidney, BC, V8L 4B2

Abstract

The use of visible-near infrared and short wave infrared spectroscopy (VNIR-SWIR) in the exploration for sediment-hosted Zn-Pb [a.k.a. SEDimentary EXhalative (SEDEX)] deposits was tested in basinal shale environments of the Howard's Pass and MacMillan Pass districts, Selwyn Basin. The Howard's Pass District hosts twelve SEDEX Zn-Pb deposits. Mineralization is hosted in Early Silurian carbonaceous and calcareous to siliceous mudstones. Mineralization is bedded, and no vent complex or strong hydrothermal alteration has been documented. The two main deposits in the MacMillan Pass District are Tom and Jason. Host rocks to the Tom deposit are interbedded chert-pebble conglomerate, diamictite, and black laminated shale and chert of the Late Devonian Lower Earn Group. Mineralization at Tom is comprised of a well-preserved vent complex and overlying bedded sulphides, and an underlying stringer zone that is comprised of veins and replacements of silica, siderite, mica, sulphides and barite. Spectra were collected from drill cores in the field using an ASD Fieldspec® Pro 3 with a contact probe. Given the high carbon and pyrite contents of the host rocks of the Howard's Pass and MacMillan Pass districts, spectra typically exhibit low reflectance and weak absorption features.

In the Howard's Pass District, footwall and hanging wall rocks are for the most part spectrally unresponsive over a 40 km-long strike length of discontinuous sulphide mineralization. One unit in the hanging wall (Flaggy Mudstone) is

Recommended citation
Peter, J.M., Layton-Matthews, D., Gadd, M.G., Gill, S., Baker, S., Plett, S., and Paradis, S., 2015. Application of visible-near infrared and short wave infrared spectroscopy to sediment-hosted zinc-lead deposit exploration in the Selwyn Basin, Yukon, *in* Paradis, S., ed., Targeted Geoscience Initiative 4: sediment-hosted Zn-Pb deposits: processes and implications for exploration; Geological Survey of Canada, Open File 7838, p. 152-172. doi:10.4095/296328

weakly spectrally responsive with scattered, weak to moderately abundant muscovite, phengite, siderite, montmorillonite, and kaolinite. The unit hosting the mineralization (Active Member) is spectrally weak to unresponsive, except in and adjacent to significant mineralization where spectral zones are comprised of siderite, montmorillonite, and phengite; these zones are also characterized by high mean spectral reflectances. Based on the Al-OH absorption feature, muscovite (2209 nanometers [nm] and below) prevails everywhere except within and immediately below the Active Member, where phengite predominates (2214 nm and higher wavelengths).

In the MacMillan Pass District, siderite, muscovite, phengite and montmorillonite are spectrally identified within the feeder zone of the Tom West deposit. At the base of the bedded sulphide-barite mineralization situated above the feeder zone, there is a 5 m-wide interval of siderite-montmorillonite that has high reflectance values. However, the immediate hanging wall and footwall rocks to mineralization (cherty carbonaceous mudstone) do not have a spectral expression.

Many of the key minerals spatially associated with the sediment-hosted Zn-Pb mineralization in the Selwyn Basin (apatite, pyrite, sphalerite, barite, K-Ba feldspar) do not have a spectral signature. However, we find that siderite, muscovite, phengite, and montmorillonite spatially associated with mineralization do have spectral signatures, but they are quite subtle. Further work is currently focused on integration of the spectral signatures with field and laboratory whole rock geochemical analyses.

Introduction

Optical spectroscopy is a non-destructive tool that can be used to analyze rocks and minerals and provide valuable information about their chemical and physical properties, including mineralogy and, in some cases mineral chemistry. Optical spectroscopic data can be collected using satellite-based, airborne, field portable ground, and laboratory spectrometers. Optical remote sensing data record the interaction of electromagnetic radiation with different elements. The electromagnetic spectrum ranges from gamma radiation at short wavelengths to long radio wavelengths. Several wavelength regions are useful for geological studies, and one of the most commonly used is the short wavelength infrared region (SWIR, 1000-2500 nm).

Hyperspectral (narrow spectral bands over a continuous spectral range) data in the visible-near infrared and short wave infrared (VNIR-SWIR) are becoming increasingly used in mineral exploration, and are particularly useful in the exploration for hydrothermal mineral deposits such as volcanogenic massive sulphide (VMS; e.g. Laakso et al., 2015; Laakso et al., in press) and orogenic

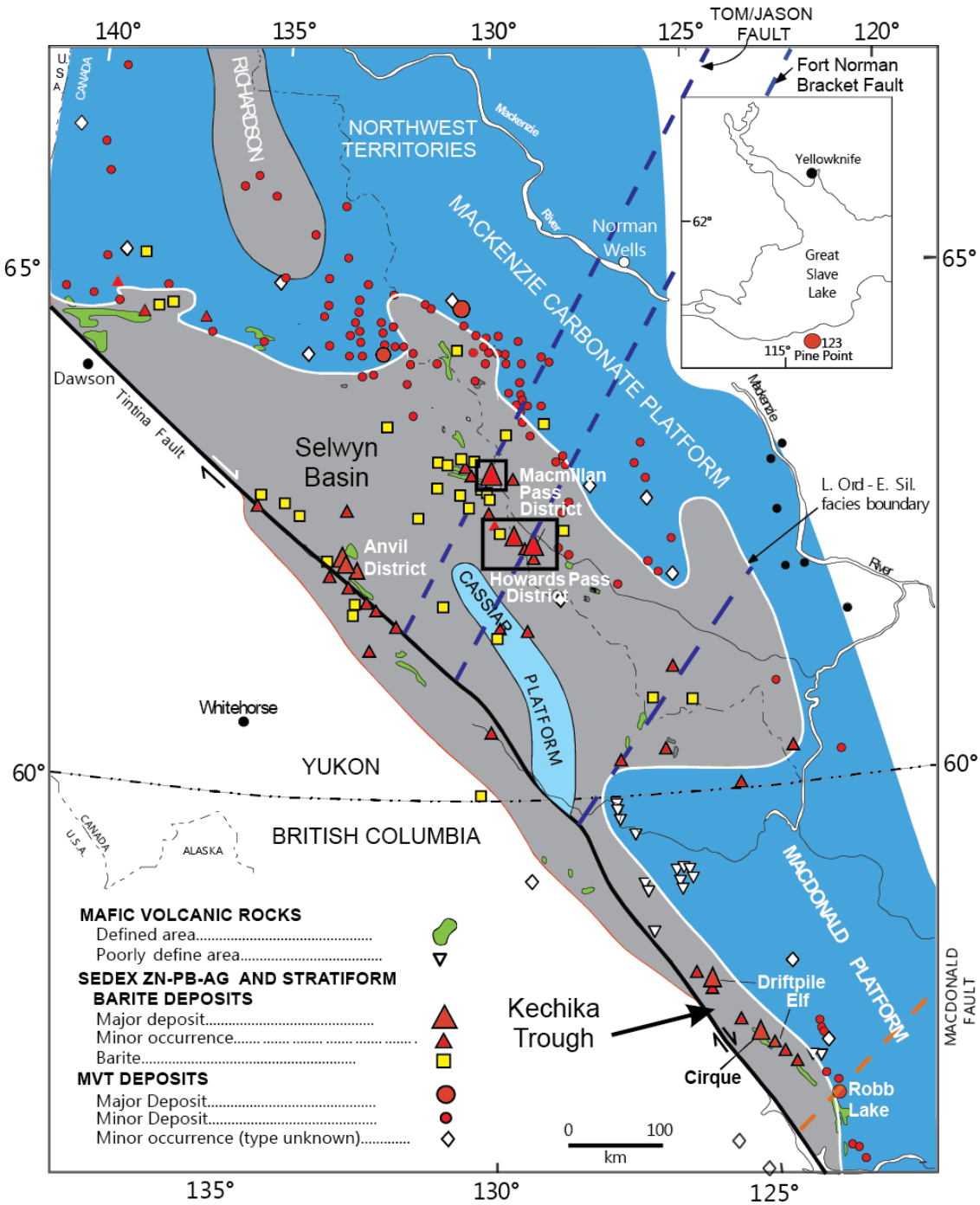

Figure 1. Map of Selwyn Basin showing the MacMillan Pass (northern box) and Howard's Pass (southern box) study areas, two of the major Zn-Pb districts within the basin (modified from Goodfellow, 2007).

and epithermal gold deposits (e.g. Bierwirth et al., 2002; Yarra et al., 2014) because the hydrothermal alteration minerals associated with these deposits (e.g. chlorite, white mica, carbonate) have characteristic spectral signatures in the SWIR (e.g. Clark et al., 2007). The application of this technology in the

exploration for sediment-hosted Zn-Pb deposits in Canada, however, remained untested to now, aside from a few measurements conducted on non-georeferenced, representative samples from the Sullivan deposit, B.C., and the Faro deposit, Anvil district, Yukon (AusSpec International Ltd., 2008). The objective of the present study was to perform such a test in basinal shale environments of the Howard's Pass District (HPD) and MacMillan Pass District (MPD), Selwyn Basin (Figure 1). This study is ancillary to that of Gadd et al. (2015), which aims to develop exploration vectors using microanalytical methods.

Geology

Howard's Pass District

There are twelve Zn-Pb SEDEX deposits in the HPD that collectively contain an estimated 393 Mt grading 4.5% Zn and 1.5% Pb (Selwyn Chihong Mining Limited, 2012). The HPD is located within the Selwyn Basin (Figure 1), a prolific metallogenic province that is primarily known for its world-class sediment-hosted Zn-Pb [a.k.a. SEDimentary EXhalative (SEDEX)] deposits. Mineralization occurs along four discrete time-stratigraphic horizons (oldest to youngest: Anvil District—Cambrian; Vulcan—Middle Ordovician; Howard's Pass District—Silurian; MacMillan Pass and Gataga districts—Devonian; Goodfellow, 2007).

Mineralization in the HPD is hosted by a sequence of carbonaceous pelagic and hemipelagic mudstone, shale and chert of the Early Silurian "Active Member" (ACTM) of the Howard's Pass (Duo Lake) Formation (Figures 3, 4, 5). Immediately overlying the ACTM (Figure 5A) is the Upper Siliceous Mudstone (USMS; Figure 5B), and above that the Upper Silurian Flaggy Mudstone Member (FLMD; Figure 5C) of the Steel Formation. Immediately below the ACTM are the Lower Cherty Mudstone (LCMS; Figure 5D) and the Calcareous Mudstone (CCMS; Figure 5E). Mineralization is bedded/laminated (where not deformed; Figure 5D), and no vent complex and/or strong hydrothermal alteration has been observed in the district. For more detail on the geology and stratigraphy of the HPD, the reader is referred to Goodfellow and Jonasson (1986).

Tom Deposit Area, MacMillan Pass District

Host rocks to the Tom deposit in the MPD (Figures 6 and 7) are interbedded chert-pebble conglomerate and chert clast grits (MCG; Figure 8A), diamictite consisting of chert pebble conglomerate, sand-striped mudstone, and mudstone clasts in a mudstone matrix (MD), black carbonaceous mudstone with light grey sand and silt interbeds (MMA; Figure 8B) and black carbonaceous siliceous mudstone and chert with pyrite and barite laminae (TCh) of the Late Devonian Lower Earn Group. Mineralization is comprised of a well-preserved vent facies complex (veins, breccias, replacements of sulphides, Fe-carbonates, and quartz) (TS; Figure 8C) and overlying interbedded barite, chert, sphalerite, galena and pyrite (TB; Figure 8D), and an underlying stringer zone that is comprised of veins and replacements of silica, siderite, mica, sulphides and barite. MMA, MCG, MD, and TCh form the stratigraphic footwall to mineralization (TB, TS), and TCh and various carbonaceous and siliceous mudstones (some radiolarian-bearing) form

the stratigraphic hanging wall. For a detailed description of the geology of the MPD, the reader is referred to Goodfellow and Rhodes (1990).

Our sampling and spectral measurement strategy was to obtain data for most proximal (feeder zone and vent complex) mineralization of the Tom West deposit (represented by drillholes TS91-014 and TYK-001) and move systematically away along-strike from the proximal to distal mineralization in drillholes TYK-004, TYK-005, TS-009, TS91-19, JS76-017, and JS76-008 (see Figure 6).

Results/Data Analysis

Methodology

The objective was to determine if there are variations in the spectral parameters that may serve as an indicator of mineralization, or a vector toward it. Spectra were systematically collected in the field from drill cores of the mineralized sequence, or favourable stratigraphy, if unmineralized, and stratigraphic hanging wall and footwall in both the HPD "Zinc Corridor" and the Tom West deposit in the MPD. Measurements were made using an ASD FieldSpec® Pro 3 (Figure 2) that records in the 350-2500 nm wavelength region with a spectral resolution of 10 nm and a sampling interval of 2 nm in the short-wave infrared wavelength region. The spectrometer was equipped with a fore optic contact probe (1 cm diameter circular field of view) to ensure consistent illumination conditions during data acquisition. Radiance values were converted to reflectance values by means of a panel of pressed polytetrafluoroethylene, commercially known as Spectralon™ (Labsphere, New Hampshire, US; Bruegge et al., 1993). Dark current and white reference measurements were repeated periodically throughout the day during data acquisition in order to ensure consistency in the spectral measurements.

Figure 2. Collecting optical reflectance spectra from drill core samples with a field portable spectrometer in the Selwyn Chihong Mining Limited Don Camp core logging and sampling facility, Howard's Pass District, Selwyn Basin, Yukon.

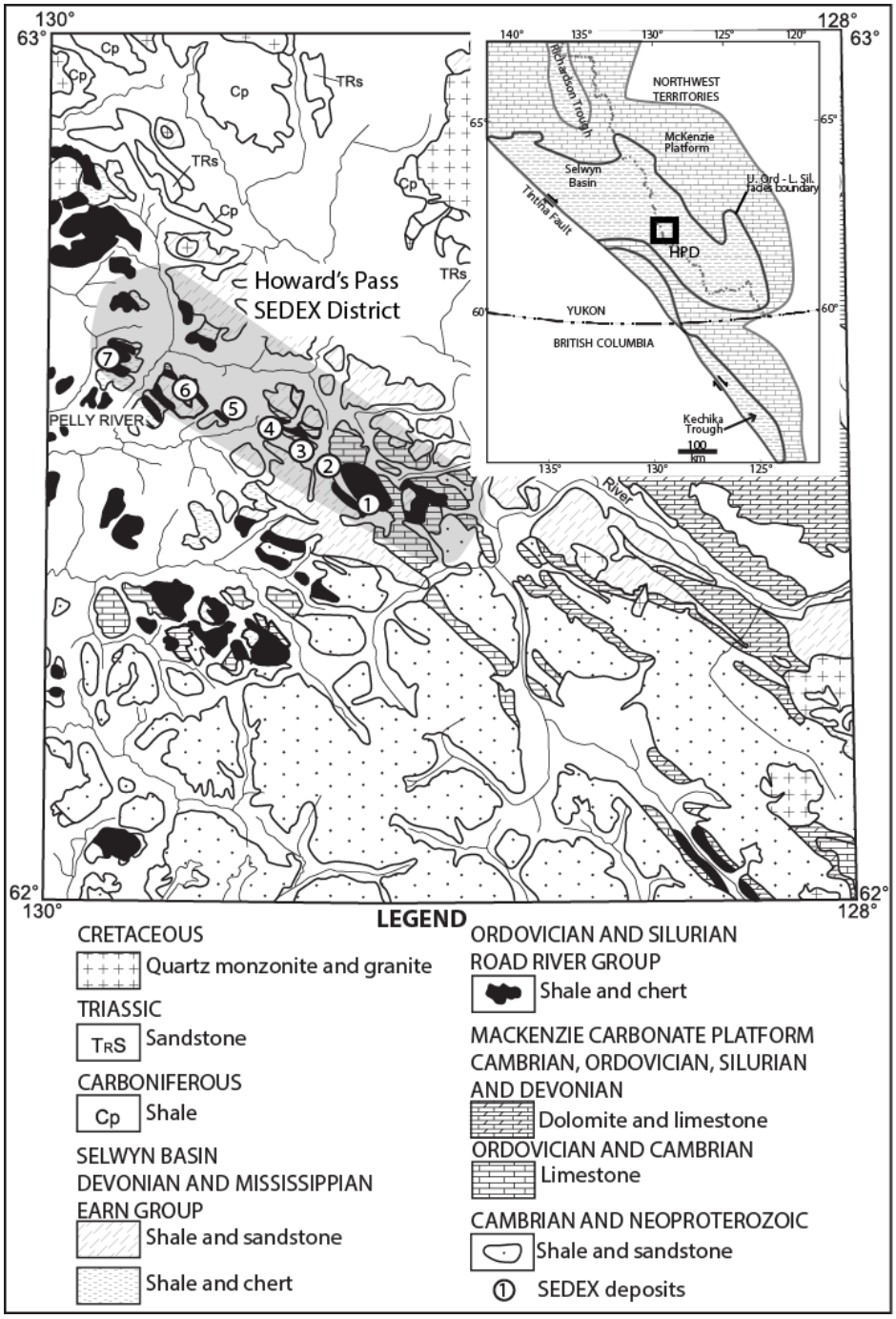

Figure 3. Regional geologic map of the Howard's Pass District (from Gadd et al., 2015). Also shown are the sediment-hosted Zn-Pb deposits and mineralized zones that define the >40 km-long "Zinc Corridor": 1: XY zone (XY, XY Central and XY West deposits); 2: Brodel deposit; 3: HC zone (HC and HC West deposits); 4: Don zone (Don and Don East deposits); 5: Anniv Zone (Anniv and Anniv East deposits); 6: OP deposit; 7: Pelly North deposit. Inset shows location of Selwyn Basin in the northern Cordillera.

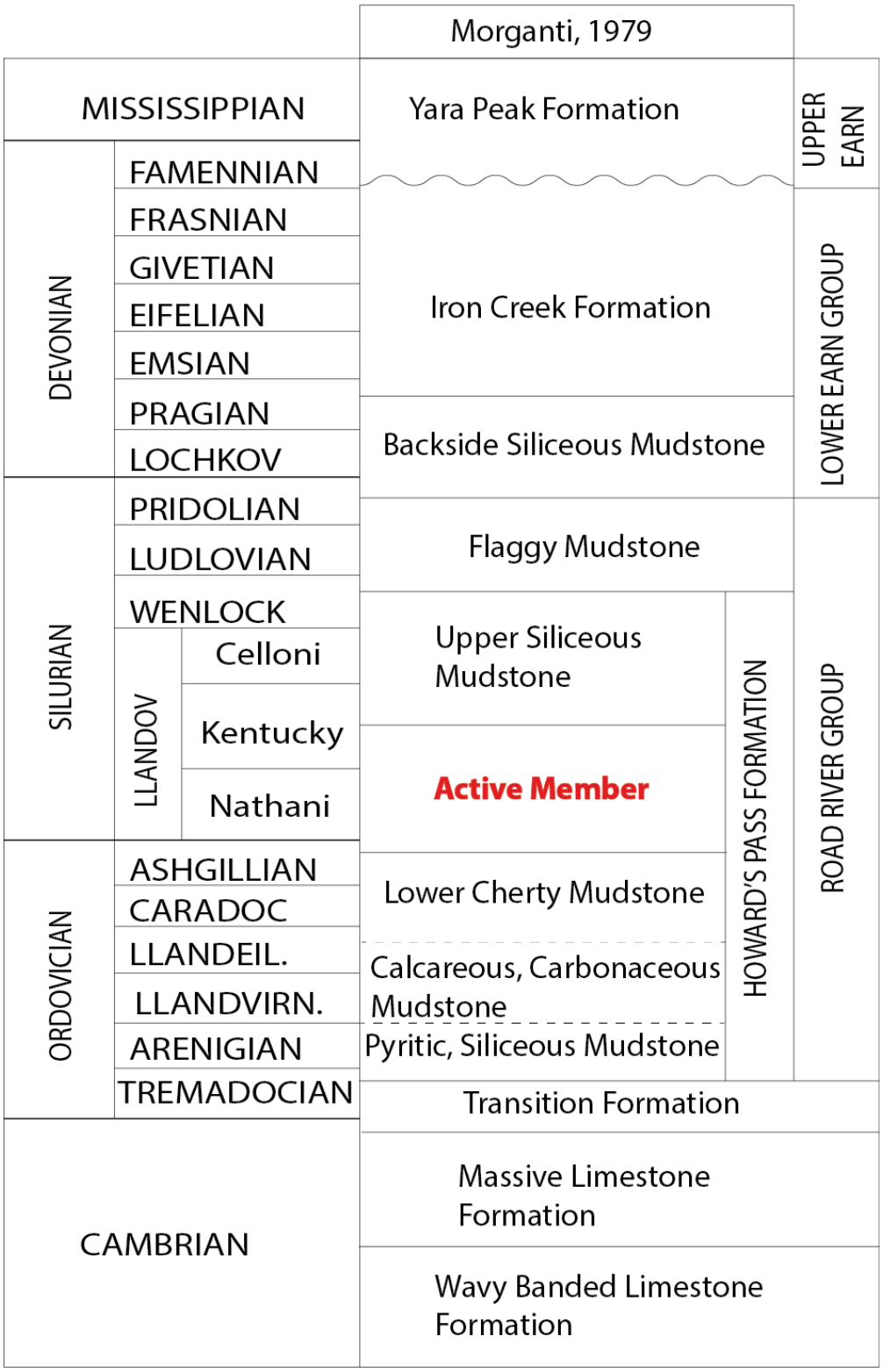

Figure 4. Stratigraphic section of the Howard's Pass District (modified from Goodfellow and Jonasson, 1986). The Active Member is the unit that hosts the mineralization.

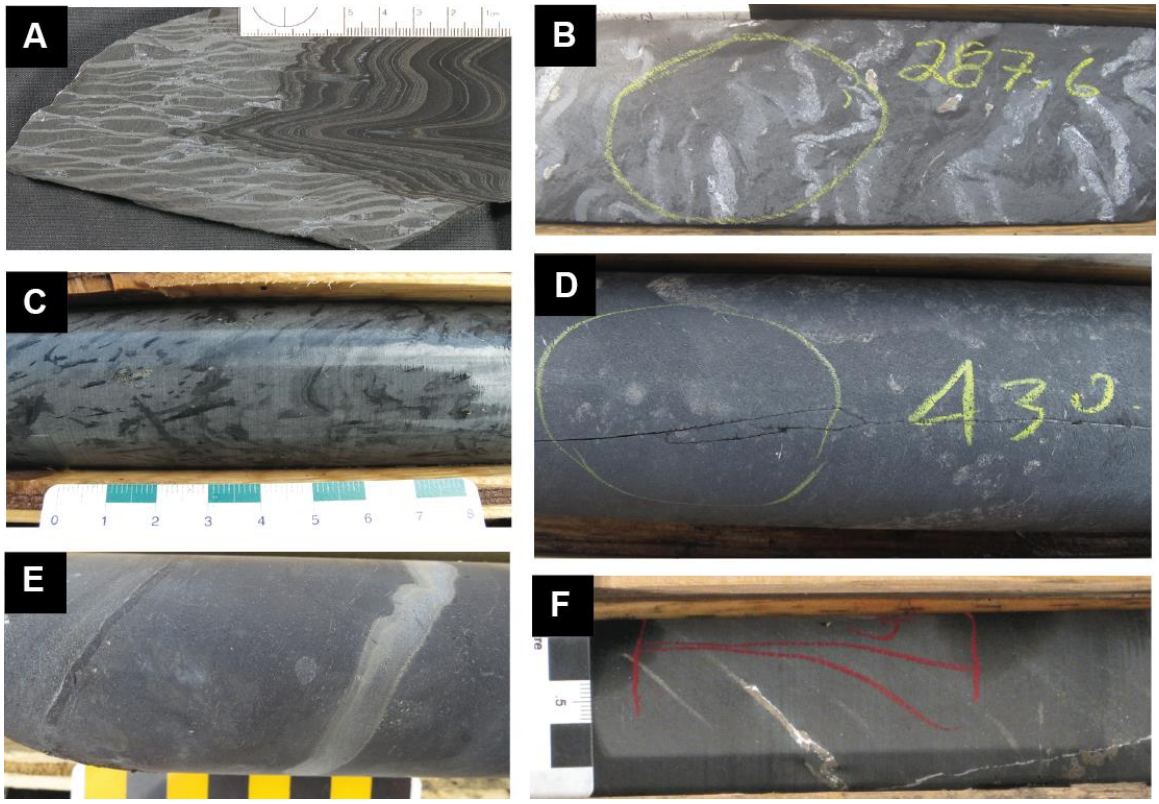

Figure 5. Drillcore photographs of representative samples from the stratigraphic succession in the Howard's Pass District. Terminology is from Morganti (1979). A) Backside Siliceous Mudstone (BSMS); B) Flaggy Mudstone (FLMD); C) Upper Siliceous Mudstone (USMS). Drillcore diameter is 4.8 cm; D) Active Member (ACTM); E) Lower Cherty Mudstone (LCMS). Drillcore diameter is 4.8 cm; F) Calcareous Carbonaceous Mudstone (CCMS).

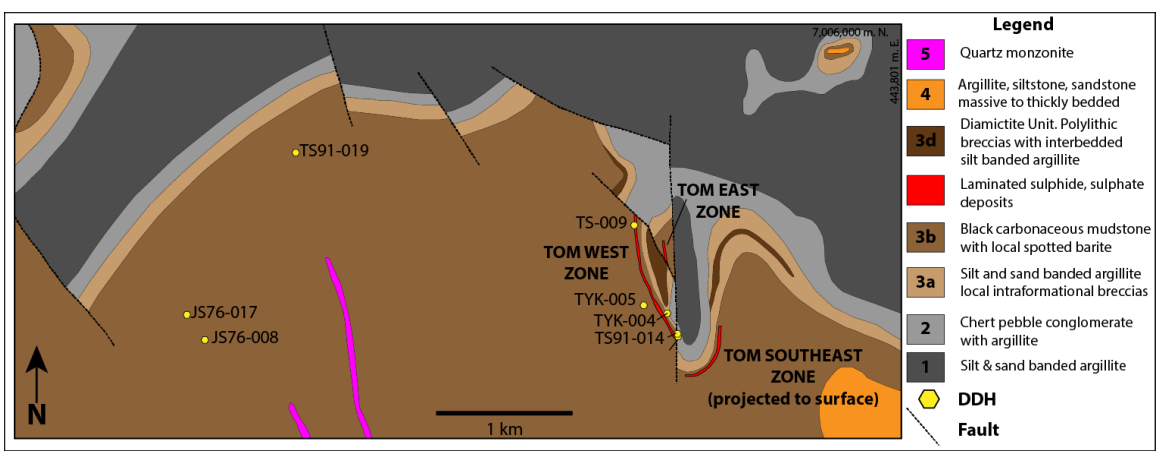

Figure 6. Geological map of the Tom deposit area, MacMillan Pass District, Selwyn Basin, Yukon (modified from Cameron, 1992). Shown are the locations of diamond-drill holes (DDH) from which systematic spectral data were collected from the mineralization (or favourable horizon) and stratigraphic footwall and hanging wall. Legend colours correspond to those in the stratigraphic section of Figure 7.

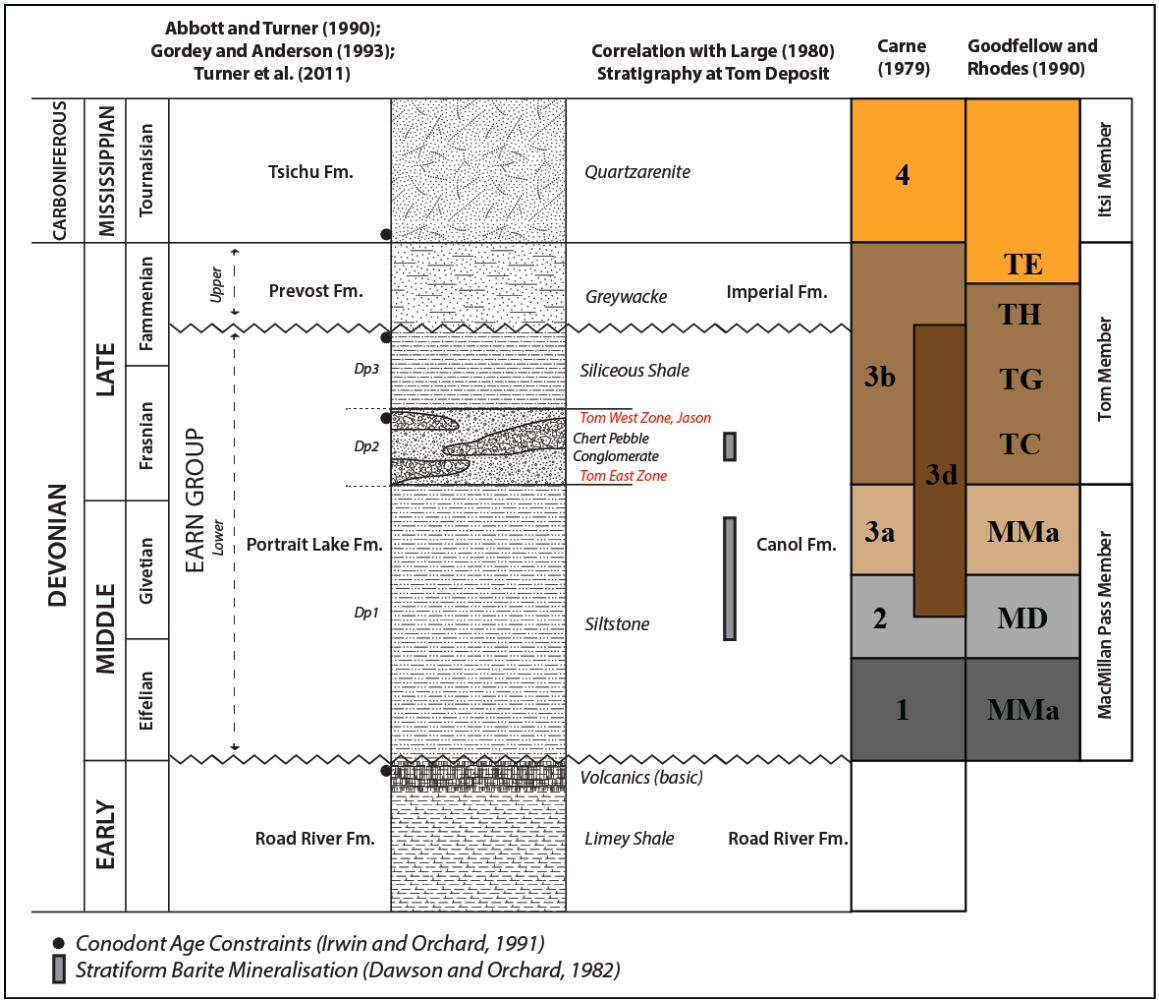

Figure 7. Stratigraphic section of the MacMillan Pass District, Yukon (modified from Magnall et al., 2014). Colours correspond to those in the geological map of Figure 6.

Given the high carbon and pyrite contents of the host rocks in both the HPD and MPD, collected spectra typically exhibit low reflectance and weak absorption features, such that absolute reflectance was used, together with a calibration file supplied by the instrument manufacturer. Additionally, a spectrum averaging value of 200 was used rather than the commonly used value of 60 for typical (i.e. more spectrally responsive) rocks. Spectral readings with low signal-to-noise ratios or failed readings were discarded. The spectra were analyzed using the "The Spectral Geologist-Core" software (TSG. version 7; AusSpec International Ltd., 2012). Spectral were hull quotient-corrected to reduce the effects of the background spectral slope when the absorption feature wavelength is to be accurately recorded (Clark and Roush, 1984). The hull quotient correction (continuum removal) is conducted by fitting straight-line segments (convex hull points) over the shoulders (maxima) of an absorption feature, and dividing the reflectance values of the absorption feature by these convex hull points. The resulting hull quotient values are normalized to a 0-1 scale hence removing the effects of albedo variance in the spectrum.

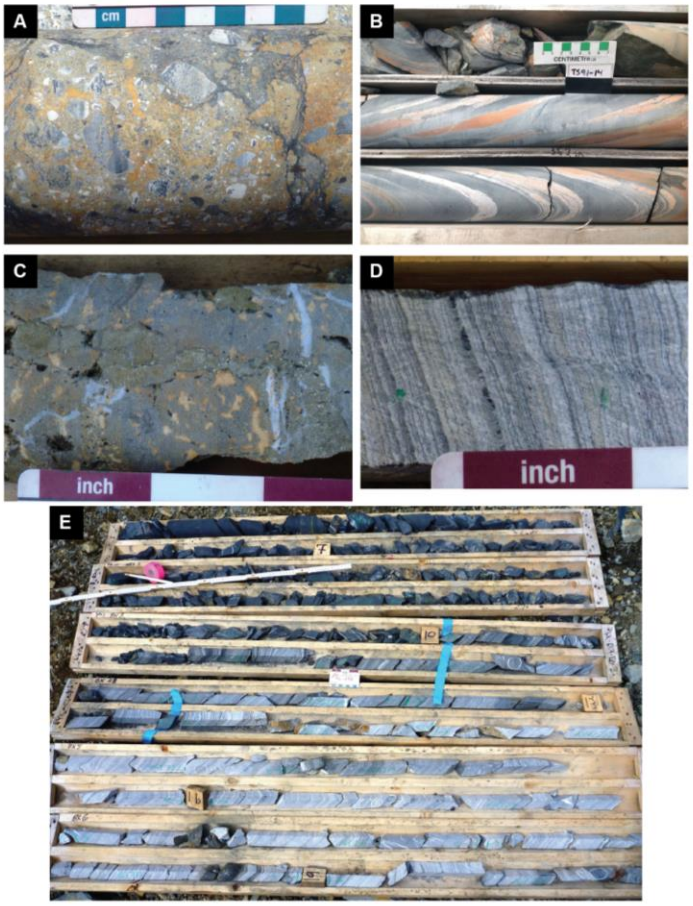

Figure 8. Drill core photographs of representative samples from the stratigraphic succession in the MacMillan Pass District. Terminology is from Goodfellow and Rhodes (1990). A) Chert pebble conglomerate (MCG) with orange weathering Fe carbonate-rich matrix (hydrothermal breccia), DDH TYK001, 078.6 m; B) Interbedded silt/sand and mudstone (MMA; footwall to mineralization) with orange weathering Fe carbonate, DDH TS91-14, 350-354 m; C) Vent complex massive sulphide (TS) with orange weathering Fe carbonate, DDH TYK001, 39.0 m; D) Bedded massive sulphide (TB), DDH TYK001, 021.5 m; E) Transition from hanging wall black carbonaceous mudstone (TCh; top 2 ½ core boxes) to bedded massive sulphides (TB; lower 3 ½ core boxes), DDH TYK001, 0-20 m.

Reflectrance Spectroscopy of the "Zinc Corridor", Howard's Pass District

In the HPD, we collected 1499 spectra from 16 drill cores along a 40 km-long strike length of discontinuous mineralization that comprises the "Zinc Corridor", extending from the XY zone (i.e. XY, XY Central and XY West deposits) in the southeast to the Pelly North deposit in the northwest (see Figure 3). Deposits and drill cores measured are as follows: XY (Central): diamond-drill holes XYC-190, XYC-208, XYC-224, XYC-243; Don: DON-076, DON-083, DON-200, DON-239; Anniv (Central): ANC-109; Anniv (East): ANE-108; Pelly North: PLN-003, PLN-005, PLN-007; OP: OPX-011, OPX-017; Brodel: BRO-010. The spectral features of the samples from these drillholes are typified by the representative

spectra shown in Figure 9A and B. Prominent absorption features occur at or around 1060, 1290, 1425, 1800, 1920, 2200, and 2330 nm, indicative of the presence of Fe-carbonates, montmorillonite, and white mica (see below).

The chemical composition of the phyllosilicate minerals may change through several substitutions such as simple Mg-Fe substitution or Tschermak substitution, in which octahedral Mg and Fe substitute for Al concurrently with tetrahedral Si for Al (Miyashiro and Shido, 1985; Guidotti and Sassi, 1998). These substitutions can be observed as spectral shifts within the Al-OH and Fe-OH absorption features near 2200 nm and 2250 nm, respectively (Clark et al., 2007). The wavelength position of the Al-OH absorption feature, present in dioctahedral muscovite, shifts systematically toward shorter wavelengths as the Al content of the octahedral sites increases, and the opposite effect, or a systematic shift toward longer wavelengths, takes place when the relative proportion of octahedral Mg and Fe increases (Post and Noble, 1993; Duke, 1994). These dioctahedral minerals form a solid solution series between paragonite, muscovite and phengite (Velde, 1965; Li et al., 1994) and are commonly termed white micas.

The chemical composition of carbonates affects their spectral response, with the prominent absorption occurring at ≈2300 nm in Mg carbonates, 2320 nm in Mg-Fe carbonates, ≈2330 nm in Fe carbonates, ≈2340 nm in Ca carbonates, 2360 nm in Mn carbonates, and ≈2400 in Zn carbonates. Ferrous iron absorptions (between ≈900 and ≈1300 nm) are common to all Fe carbonates (ankerite, siderite, Fe-calcite), and their intensity varies with Fe content. In practice, determination of siderite is difficult due to the variable Mg and Fe content possible in carbonates. The presence of siderite in the HPD was confirmed based on the presence of absorption features at 2330, 1060 and 1290 nm.

Montmorillonite (Al-smectite) has absorptions at ≈1400, 1800, ≈1900, and ≈2200 nm, and is distinguished from illite in that the former does not have the secondary Al-OH absorption features at 2360 and 2450 nm typically present in illite. Montmorillonite is distinguished from kaolinite in that the former does not have a 2160 nm absorption feature. On this basis, montmorillonite is identified in the spectra of the HPD.

The ACTM which hosts Zn-Pb mineralization at HPD is generally spectrally weak to unresponsive, except in and adjacent to significant sulphide mineralization where spectral zones are comprised of siderite (evidenced by prominent absorption features around 1060 nm, 1290 nm and a less pronounced absorption around 2330 nm), montmorillonite (evidenced by a prominent absorption features around 1800 nm, but without the characteristic secondary Al-OH absorption features at 2360 and 2450 nm), and white mica (phengite, as evidenced by the wavelength of the prominent Al-OH absorption feature around 2200 nm) (Figure 9A). These zones are also characterized by high mean spectral reflectances. The

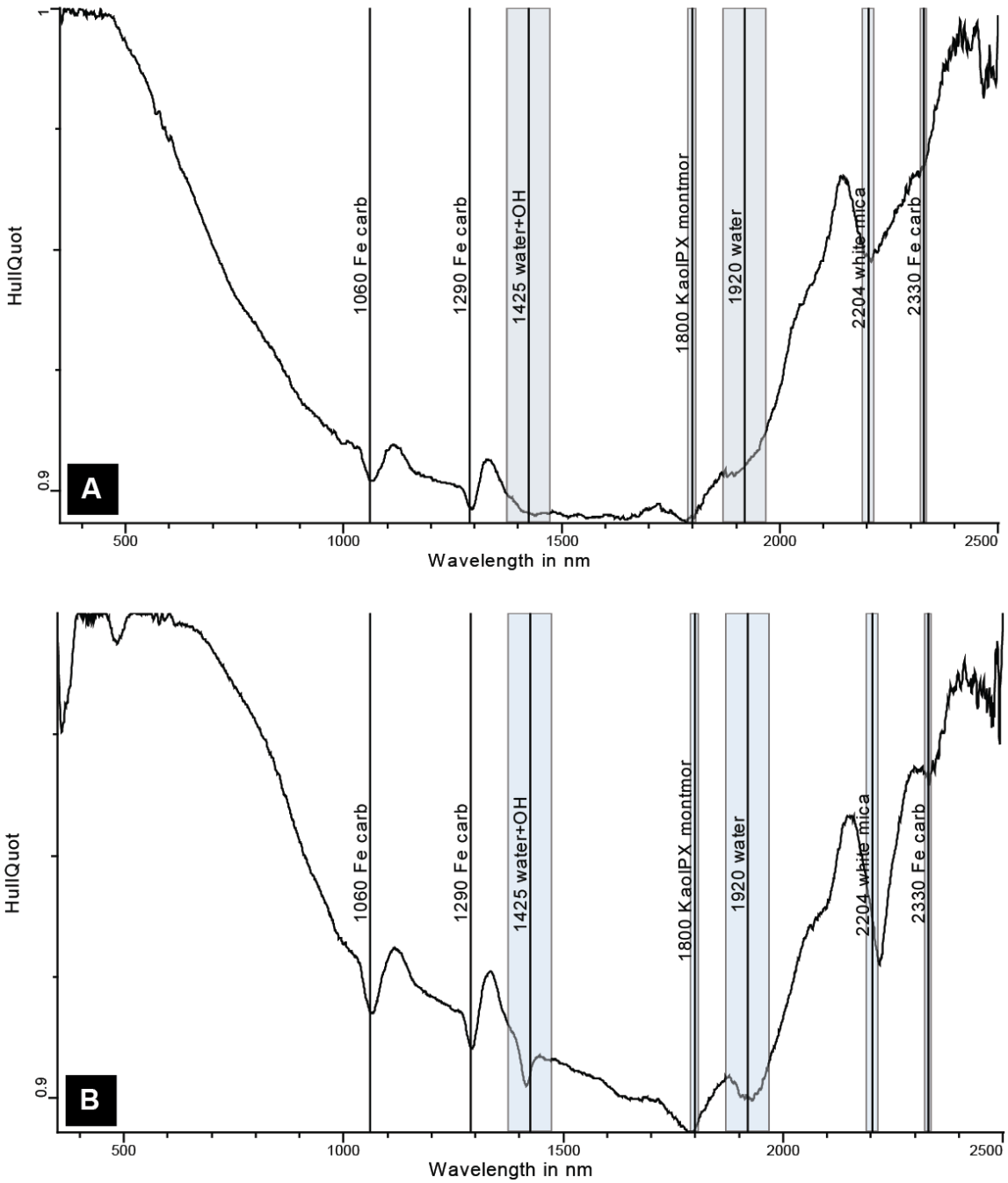

Figure 9. A) Representative hull quotient reflectance spectral plot from lower part of the mineralized Active Member (ACTM), Howard's Pass District, DDH XYC-224 (XY Central deposit), 186.2m. Absorption features indicate the presence of white mica, Fe carbonate, and montmorillonite. In many samples, Fe carbonate is not identified in the spectra; B) Representative hull quotient reflectance spectral plot from Flaggy Mudstone (FLMD), Howard's Pass District, DDH DON-76 (Don East deposit), 108.2m. Absorption features indicate the presence of white mica, Fe carbonate, and montmorillonite. Abbreviations: Fe carb = Fe carbonate; KaolP X montmor = kaolinite/montmorillonite.

USMS (unit immediately above the ACTM), LCMS (unit immediately below the ACTM) and CCMS (unit immediately below the LCMS) are, for the most part, spectrally unresponsive. The FLMD generally is weakly spectrally responsive with scattered, little to moderately abundant muscovite, phengite, siderite, montmorillonite, and kaolinite (all evidenced by the absorption features outlined above) (Figure 9B).

The composition of white mica can be determined by using the wavelengths of the Al-OH absorption feature that varies depending on the octahedral Al content. Variation occurs in the following manner: paragonite (Na-sericite; high Al) 2180-2190 nm; muscovite ("normal" potassic) 2200-2210 nm; phengite (Mg-Fe substituted; low Al) 2216-2228 nm. Using these criteria, phengite (higher wavelengths) predominates within and immediately below the ACTM, and muscovite (2209 nm and below) prevails elsewhere (Figure 10A).

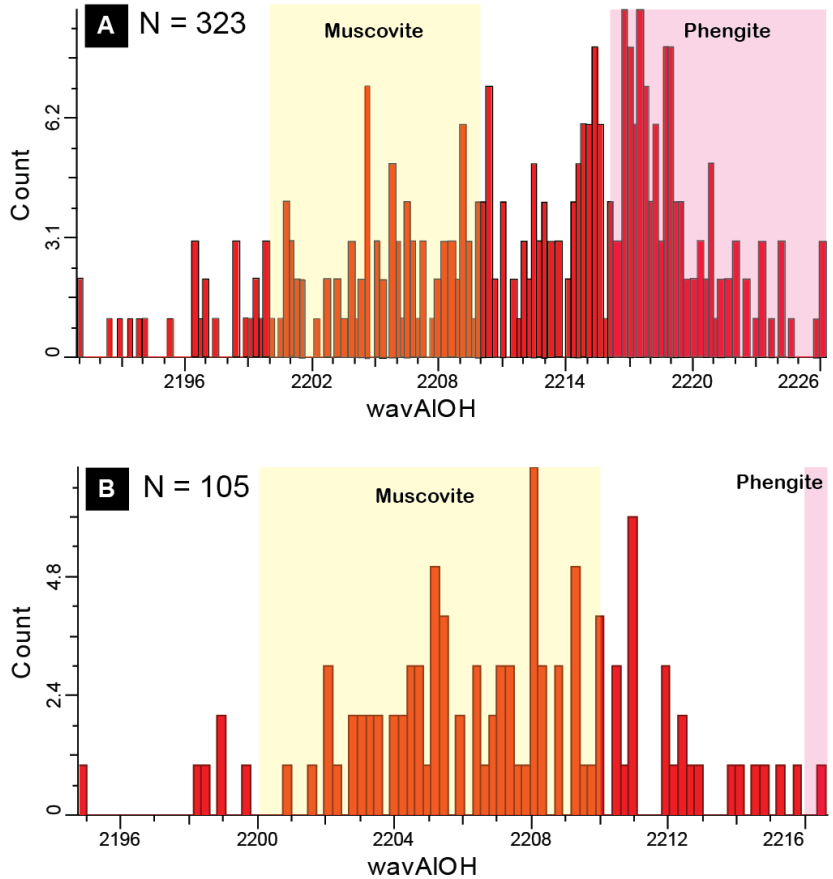

Figure 10. A) Histogram of Al-OH absorption wavelengths in DDH XYC-190 (XY Central deposit). There are two compositional ranges in white micas from muscovite (2200-2210 nm; shown in yellow) to phengite (2216-2228 nm; shown in pink), with the latter associated with the Active Member (ACTM); B) histogram of Al-OH absorption wavelengths in DDH TS91-14, MacMillan Pass District. A single population shows compositional variation in white micas that ranges from muscovitic to phengitic, with most being muscovitic (2200-2210 nm).

Reflectrance Spectroscopy of the Tom West Deposit, MacMillan Pass District

We collected 313 spectra from 4 drill cores extending from the core of the Tom West deposit (TYK-001 and TS91-14) up to 400 m away along strike (TYK-004 and TYK-005). We also collected additional data from drill cores that are even more distal from mineralization (TS-91-019, JS76-017, JS76-008, TS-009; Figure 6), but these have not yet been analyzed. At the base of (and within) the sulphide-barite bedded mineralization, situated immediately above the feeder zone, there is a 5 m-wide interval of siderite-montmorillonite that has high reflectance values. Siderite is evidenced by prominent absorption features around 1060 nm and1290 nm (and the characteristically shaped trough formed by them) and a less pronounced absorption around 2330 nm. Montmorillonite is characterized by a subtle absorption feature around 1800 nm, but without the secondary Al-OH absorption features at 2360 and 2450 nm (Figure 11A). Siderite, muscovite (Al-OH absorption feature at 2209 nm and below), phengite (Al-OH absorption feature range from 2216 to 2228 nm) and montmorillonite (absorptions at 1800 and 1920 nm, but not at 2160, 2360 and 2450 nm) are spectrally identified within the feeder zone (MCG, MD, MMA) (Figure 11B).

However, the immediate hanging wall and footwall rocks to Pb-Zn-Ba mineralization (cherty carbonaceous mudstone; TC) do not have a spectral expression. Al-OH absorption wavelengths, which are a robust indicator of white mica composition, show a single population, with a compositional range from muscovitic to phengitic, with muscovitic compositions predominating (Figure 10B).

Discussion/Models

Reflectance parameters vary between the various host lithologies of deposits of the HPD and the Tom West deposit in the MPD, but there are no systematic discernable variations that can be used to unambiguously indicate proximity to mineralization or vector toward it. In the HPD, calculations of the white mica crystallinity index ([depth of Al-OH absorption feature at 2200 nm] / [depth of water absorption feature at 1900 nm]) for almost all drill cores shows no systematic variation within and between the stratigraphic units. Calculations of the depth of the Al-OH absorption feature for almost all drill cores in the HPD shows no systematic variations that can be used to indicate proximity to mineralization or vector toward it. However, in several drill cores (AN-108 from the Anniv deposit, DON-76 from the Don deposit, and OP-17 from the OP deposit) values are at their maxima in the immediate footwall to sulphide mineralization. At the Tom West deposit, the values for the depth of the Al-OH absorption feature are highest in the carbonaceous mudstone that is the immediate footwall (drill cores TYK-001 and TYK-005) and hanging wall to sulphide-barite mineralization (drill core TYK-004).

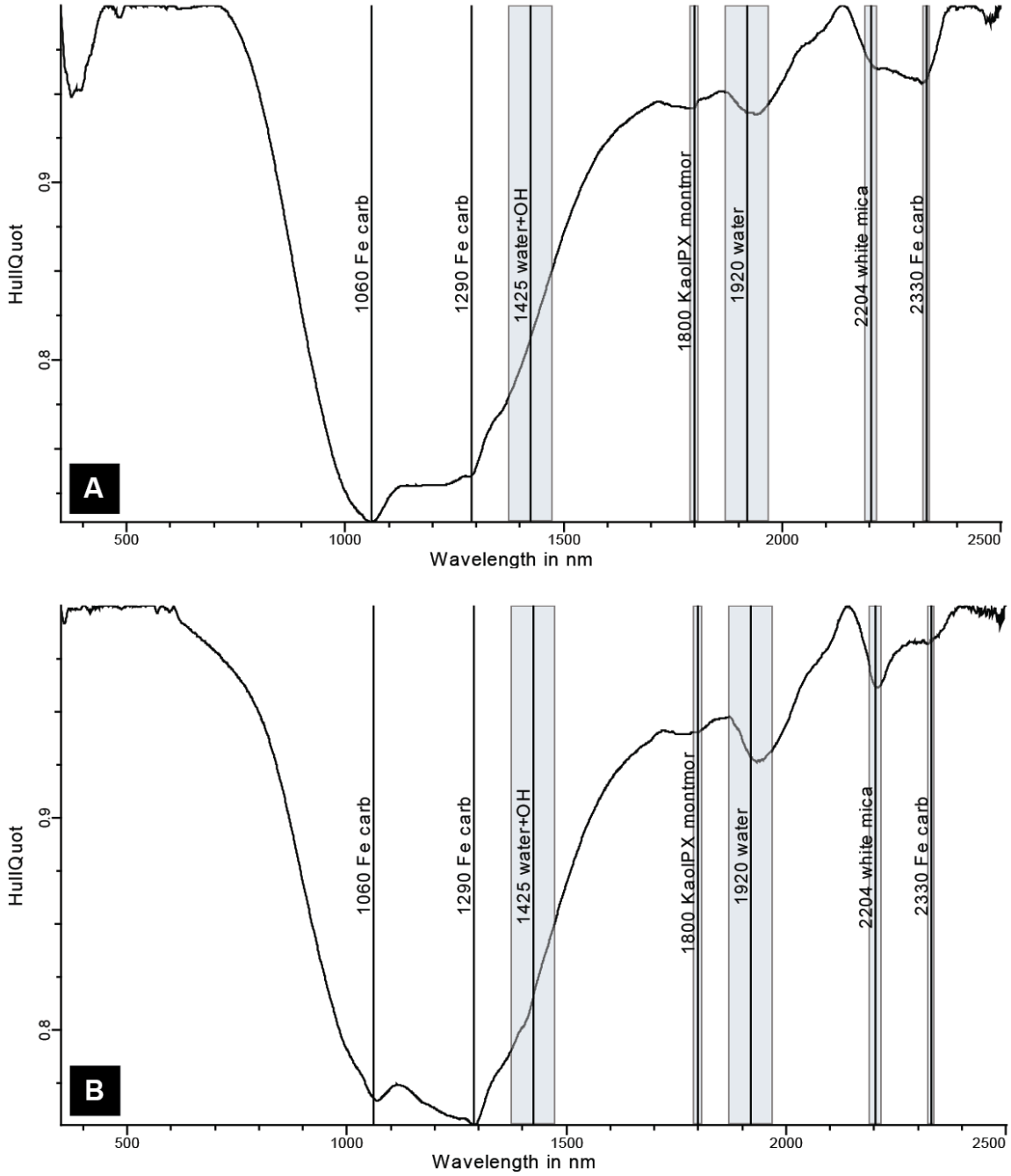

Figure 11. A) Representative hull quotient reflectance spectra from bedded massive sulphide (TB) with minor carbonaceous mudstone laminae (TC), MacMillan Pass District DDH TYK-001, 034.2m. Absorption features indicate the presence of white mica (muscovitic), Fe carbonate (siderite), and very minor montmorillonite; B) Representative hull quotient reflectance spectra from feeder zone (quartz-siderite veins and replacements) in chert pebble conglomerate (MCG), MacMillan Pass District, DDH TYK-001, 078.6m. Absorption features indicate the presence of white mica (muscovitic), Fe carbonate (siderite), and very minor montmorillonite. Abbreviations: Fe carb = Fe carbonate; KaolP X montmor = kaolinite/montmorillonite.

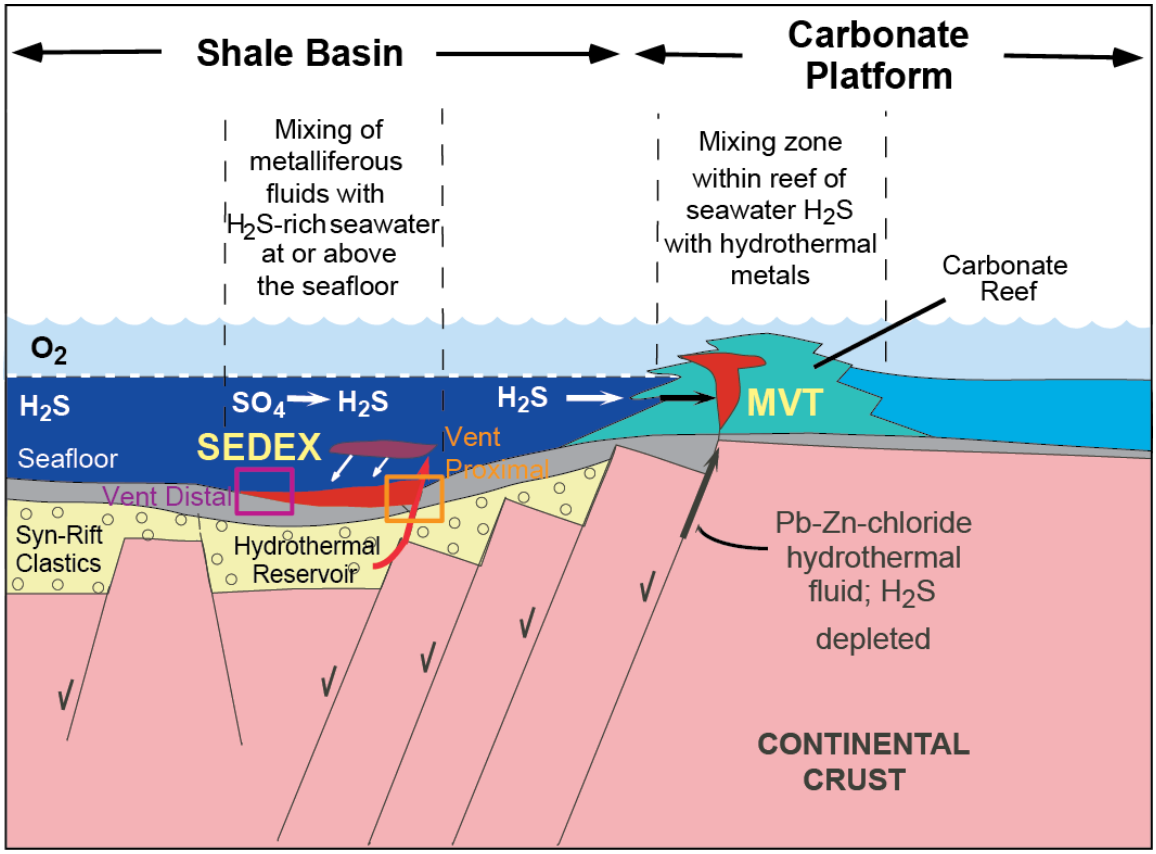

Figure 12. Genetic model for formation of sediment-hosted Zn-Pb and coeval Mississippi Valley-type (MVT) deposits in Selwyn Basin (from Goodfellow, 2007). Note the relative positions (no scale implied) of vent-proximal sediment-hosted Zn-Pb deposits such as Tom West in the MacMillan Pass District (orange box) and vent-distal sediment-hosted Zn-Pb deposits such as those (XY, Brodel, Don, HC, Anniv, OP, Pelly North) of the "Zinc Corridor" in the Howard's Pass District (purple box). Vent-proximal deposits are situated over a vent complex, whereas vent-distal deposits are situated far from the site of the venting fluids.

The Zn-Pb-Ba mineralization in the MPD (Tom and Jason deposits) were interpreted by Goodfellow and Rhodes (1990) and Goodfellow (2007) as vent-proximal deposits (see orange coloured box in Figure 12), whereas the Zn-Pb deposits along the HPD "Zinc Corridor" were interpreted as vent-distal (no feeder systems have been identified) deposits (Goodfellow, 2007; see purple coloured box in Figure 12). Note that Figure 12 is a schematic representation of one mineralizing event (horizon), whereas there are four known such horizons, and the deposits of the MPD and HPD actually occur at different horizons. Nevertheless, in the MPD, spectrally responsive vent-related hydrothermal alteration minerals may potentially be recognized, together with spectrally responsive minerals within the mineralization (that formed in the water column or diagenetically from pore waters in the sediments). However, in the HPD only the latter are expected. Our data show that in the MPD, siderite is a spectrally

responsive vent-related mineral, but it is ubiquitous in the sediments up to at least 400 m from the vent site. Further, siderite is also present in vent-distal mineralization within the HPD. On this basis, the spectral recognition of siderite cannot be used to vector toward mineralization.

In order to determine whether (dark grey to black) carbonaceous matter within the host units and mineralization suppresses reflectance, the following calculation (S. Pontual (Principal Geologist, AusSpec International), pers. comm., 2013) was made: [2100 nm mean reflectance value] / [600 nm mean reflectance value]. The basis for this is that in the samples measured, white mica is the dominant highly reflective mineral, and the ratio of the dominant Al-OH absorption at 2100 nm to reflectance at a wavelength where none of the diagnostic features of white mica occur (600 nm) provides a good measure of the brightness or reflectance. In some drill cores, such as DON-200 from the Don deposit, AN-108 from the Anniv deposit, XYC-190 and XYC-224 from the XY (Central) deposit, maximum values occur within the ACTM. At the Tom West deposit, maxima occur within the massive sulphide mineralized intervals (TB, TS) in drill cores TYK-001, TYK-004, and TYK-005. However, the spectral proxy for the carbonaceous matter content does not vary systematically in a manner that can be used to vector toward mineralization.

Based on the Al-OH absorption feature wavelengths, along the “Zinc Corridor” of the HPD, phengite (2216 to 2228 nm) predominates within and immediately below the ACTM, and muscovite (2209 nm and below) prevails elsewhere. Phengitic mica can form from high temperature (250-350°C) from hydrothermal fluids (Hulen and Nielson, 1986), but this temperature range is deemed too high for the mineralizing fluids in the HPD, based on metal solubility considerations (Lydon, 1983). Another influence on the chemical composition of white micas is the chemical composition of the hydrothermal fluids (Cathelineau, 1988). Elevated Mg^{2+} and Fe^{2+} (relative to Al^{3+}) contents of the hydrothermal fluid favor the formation of phengite (Yang et al., 2011). Therefore, the presence of phengitic mica immediately beneath the ACTM could reflect the greater availability of Fe than elsewhere in the host rocks of the HPD.

In the Tom West deposit area, the Al-OH absorption feature wavelengths show a single population, with a compositional range from muscovitic to phengitic, with muscovitic compositions predominating. As mentioned above, the formation of phengitic over muscovitic mica can be controlled by fluid temperature and/or fluid chemistry. However, muscovitic through phengitic white mica compositions are identified in the feeder zone at Tom West and there appears to be no systematic spatial variation/zonation that can be used for vectoring. Fluid inclusion homogenization temperatures in the hydrothermal vents at Tom and Jason (≈250°C; Gardner and Hutcheon, 1985; Ansdell et al., 1989) fall within the temperature range for phengite formation, as discussed above, but the chemical composition of the fluids may also have governed the formation of phengite over muscovite.

Conclusions

Many of the key minerals spatially associated with sediment-hosted Zn-Pb mineralization in the Selwyn Basin (apatite, pyrite, sphalerite, barite, K-Ba feldspar) do not have spectral signatures in the VNIR-SWIR portion of the electromagnetic spectrum. However, our data indicate that other minerals that are spatially associated with mineralization (siderite, muscovite, phengite, and montmorillonite) do have spectral signatures, although they are quite muted. Our data broadened a very minimal publicly available dataset, and will be useful to compare with similar datasets that may be collected elsewhere in the Selwyn Basin, or may be made available in the future.

Implications for Exploration

The sediment-hosted Zn-Pb deposits of the HPD and MPD clearly have less pronounced hydrothermal alteration signatures than Australian Proterozoic examples hosted by calcareous sediments (Large et al., 2005), and which have more pronounced spectral signatures (AusSpec International Ltd., 2008). Our work to date show that hyperspectral optical reflectance spectroscopy will be of limited use in delineating favourable horizons and vectoring toward mineralization along them in both the HPD and MPD of the Selwyn Basin.

Future Work

Further work is currently focused on analysis of additional spectral measurements made distal (further than 400 m away) from the Tom West deposit and incorporating these data into the dataset presented here. These spectral analyses will be integrated with field portable x-ray fluorescence and laboratory whole rock geochemical data to develop geochemical exploration vectors focused on “ore” and pathfinder metals, and redox sensitive elements indicative of ambient conditions.

Acknowledgements

We gratefully acknowledge the logistical and in-kind support provided by Selwyn Resources Ltd., Selwyn-Chihong Mining Ltd., HudBay Minerals Inc., and Mercer Contracting. Discussions with Wayne Goodfellow (Geological Survey of Canada; GSC) regarding the geology and geochemistry of the SEDEX deposits in both the HPD and MPD were very helpful. We also thank Sasha Pontual, AusSpec International Ltd. for input on SWIR data analysis of our data and Jeff Harris (GSC) for reviewing this contribution.

References

Abbott, J.G., and Turner, R.J.W., 1990, Character and paleotectonic setting of Devonian stratiform sediment-hosted Zn, Pb, Ba deposits, MacMillan Fold Belt, Yukon, *in* Abbott, J. G., and Turner, R. J. W., ed., Mineral deposits of the northern Canadian Cordillera (Eighth Symposium Field Trip 14 Guidebook): Ottawa, International Association on the Genesis of Ore Deposits, p. 99-136.

Ansdell, K.M., Nesbitt, B.E., and Longstaffe, F.J., 1989, A fluid inclusion and stable-isotope study of the Tom Ba-Pb-Zn deposit, Yukon Territory, Canada: Economic Geology, v. 84, p. 841-856.

AusSpec International Ltd., 2012, The Spectral Geologist Pro, v. 7.1; URL: http://www.thespectralgeologist.com/tsg_pro.htm

AusSpec International Ltd., 2008, GMEX Spectral analysis guides for mineral exploration, sedimentary exhalative deposits, v. 9, 3rd edition, 39 p.

Bierwirth, P., Huston, D., and Blewett, R., 2002, Hyperspectral mapping of mineral assemblages associated with gold mineralization in the Central Pilbara, Western Australia: Economic Geology, v. 97, p. 819-826.

Bruegge, C.J., Stiegman, A.E., Rainen, R.A., and Springsteen, A.W., 1993, Use of Spectralon as a diffuse reflectance standard for in-flight calibration of earth-orbiting sensors: Optical Engineering v. 32, p. 805-814.

Cameron, R.S., 1992, Assessment report on the 1991 diamond drill program, Jason Property, MacMillan Pass, Yukon, Canada, Mayo Mining Division: Vancouver, B.C., unpublished report for Phelps Dodge Corporation of Canada, Ltd., 122 p.

Carne, R.C., 1979, Upper Devonian stratiform barite-lead-zinc-silver mineralization at Tom claims, MacMillan Pass, Yukon Territory: Unpublished M.Sc. thesis, University of British Columbia, 149 p.

Cathelineau, M., 1988, Cation site occupancy in chlorites and illites as a function of temperature: Clay Minerals, v. 23, p. 471–485.

Clark, R., and Roush, T., 1984, Reflectance spectroscopy: quantitative analysis techniques for remote sensing applications: Journal of Geophysical Research, v. 89, p. 6329–6340.

Clark, R., Swayze, G., Wise, R., Livo, E., Hoefen, T., Kokaly, R., and Sutley, S., 2007, USGS digital spectral library splib06a: United States Geological Survey, Digital Data Series 231 (http://speclab.cr.usgs.gov/spectral.lib06).

Dawson, K.M., and Orchard, M.J., 1982, Regional metallogeny of the northern Cordillera: biostratigraphy, correlation and metallogenic significance of bedded barite occurrences in eastern Yukon and western District of Mackenzie: Geological Survey of Canada Paper 82-1C, p. 31-38.

Duke, E., 1994, Near infrared spectra of muscovite, Tschermak substitution, and metamorphic reaction progress: Implications for remote sensing: Geology, v. 22, p. 621–624.

Gadd, M.G., Layton-Matthews, D., Peter, J.M., and Paradis, S., 2015, In situ trace element and sulphur isotope analyses of pyrite constrain timing of mineralization and sources of sulphur in the Howard's Pass SEDEX Zn-Pb District, Yukon, *in* Paradis, S., ed., Targeted Geoscience Initiative 4: sediment-hosted Zn-Pb deposits: processes and implications for exploration: Geological Survey of Canada Open File, 7838, p. 58-74.

Gardner H.D., and Hutcheon, I., 1985, Geochemistry, mineralogy, and geology of the Jason Pb-Zn deposits, MacMillan Pass, Yukon, Canada: Economic Geology, v. 80, p. 1257–1276.

Goodfellow, W.D., 2007, Base metal metallogeny of the Selwyn Basin, Canada, *in* Goodfellow, W.D., ed., Mineral deposits of Canada: A synthesis of major deposit-types, district metallogeny, the evolution of geological provinces, and exploration methods: Geological Association of Canada, Mineral Deposits Division, Special Publication No. 5, p. 553-579.

Goodfellow, W.D., and Jonasson, I.R., 1986, Environment of formation of the Howards Pass (XY) Zn-Pb deposit, Selwyn Basin, Yukon, *in* Morin, J. A., ed., Mineral deposits of northern Cordillera: Canadian Institute of Mining and Metallurgy, Special Volume 37, p. 19-50.

Goodfellow, W.D., and Rhodes, D., 1990, Geology, geochemistry and origin of the Tom stratiform Zn-Pb-Ag-barite deposits, *in* Abbott, J. G., and Turner, R. J. W., ed., Mineral deposits of the northern Canadian Cordillera, Yukon and Northeastern British Columbia (Field Trip Guidebook 14): Ottawa, 8th International Association on the Genesis of Ore Deposits Symposium, p. 177-242.

Gordey, S.P., and Anderson, R.G., 1993, Evolution of the northern Cordillera miogeocline, Nahanni map area (105I), Yukon and Northwest Territories: Geological Survey of Canada Memoir, v. 428, 214 p.

Guidotti, C., and Sassi, F., 1998, Petrogenetic significance of Na-K white mica mineralogy: Recent advances for metamorphic rocks: European Journal of Mineralogy, v. 10, p. 815–854.

Hulen, J., and Nielson, D., 1986, Hydrothermal alteration in the Baca geothermal system, Redondo Dome, Valles Caldera, New Mexico: Journal of Geophysical Research, v. 91, p. 1867– 1886.

Irwin, S.E.B., and Orchard, M.J., 1991, Upper Devonian-Lower Carboniferous conodont stratigraphy of the Earn Group and overlying units, northern Canadian Cordillera: Geological Survey of Canada Bulletin 417, p. 185-213.

Laakso, K., Rivard, B., and Peter, J.M., 2015, Hyperspectral eflectance spectrometry in the exploration for VMS deposits using the Izok lake Zn-Cu-Pb-Ag deposit, Nunavut as a test site, *in* Peter, J. M., and Mercier-Langevin, P., ed., Targeted Geoscience Initiative 4: Contributions to the understanding of volcanogenic massive sulphide deposit genesis and exploration methods development: Geological Survey of Canada, Open File 7853.

Laakso, K., Rivard, B., Peter, J., White, H., Maloley, M., Harris, J., and Rogge, D., in press, Application of airborne, laboratory and field hyperspectral methods to mineral exploration in the Canadian Arctic: recognition and characterization of volcanogenic massive sulphide-associated hydrothermal alteration in the Izok Lake deposit area, Nunavut, Canada: Economic Geology.

Large, D.E., 1980, Geological parameters associated with sediment-hosted, submarine exhalative Pb-Zn deposits: an empirical model for mineral exploration: Geologisches Jahrbuch, v. D40, p. 59-129.

Large, R.R., Bull S.W., McGoldrick, P.J., Walters S., Derrick G.M., and Carr G.R., 2005, Stratiform and stratabound Zn-Pb-Ag deposits in Proterozoic sedimentary basins, northern Australia, *in* Hedenquist J.W., Thompson J.F.H., Goldfarb R.J., and. Richards, J.P., ed., Economic Geology, 100th anniversary volume, 1905-2005: Littleton, CO, Society of Economic Geologists, p. 931-963.

Li, G., Peacor, D.R., Merriman, R.J., and Roberts, B., 1994, The diagenetic to low-grade metamorphic evolution of matrix white micas in the system muscovite-paragonite in a mudrock from Central Wales: Clays and Clay Minerals v. 42, p. 369-381.

Lydon, J.W., 1983, Chemical parameters controlling the origin and deposition of sediment-hosted stratiform lead-zinc deposits, *in* Sangster, D.F., ed., Short course in sediment-hosted stratiform lead-zinc deposits: Mineralogical Association of Canada, Short Course Handbook, v. 8, p. 175-250.

Magnall, J.M., Gleeson, S.A., and Paradis, S, 2014, SEDEX mineralisation, MacMillan Pass (YT): Petrography, mineralogy and bulk geochemistry of the Tom and Nidd deposits: Geological Survey of Canada, Open File 7457, 37 p.

Miyashiro, A., and Shido, F., 1985, Tschermak substitution in low- and middle-grade pelitic schists: Journal of Petrology, v. 26, p. 449–487.

Morganti, J.M., 1979, The geology and ore deposits of the Howards Pass area, Yukon and Northwest Territories: the origin of basal sedimentary stratiform sulphide deposits: Unpub. Ph.D. thesis, University of British Columbia, 351 p.

Post, J., and Noble, P., 1993, The near-infrared combination band frequencies of dioctahedral smectites, micas, and illites: Clays and Clay Minerals, v. 41, p. 639–644.

Selwyn Chihong Mining Limited, 2012, Selwyn announces updated mineral resource for XY West deposit: Vancouver, British Columbia, Canada, Press Release, 5 p.

Turner, E.C., 2011, Stratigraphy of the Mackenzie Mountains supergroup in the Wernecke Mountains, Yukon, *in* MacFarlane, K.E., Weston, L.H., and Relf, C., ed., Yukon Exploration and Geology 2010: Whitehorse, YT, Yukon Geological Survey, p. 207-231.

Velde, B., 1965, Phengite micas: Synthesis, stability, and natural occurrence: American Journal of Science, v. 263, p. 886-913.

Yang, K., Huntington, J., Gemmell, J., and Scott, K., 2011, Variations in composition and abundance of white mica in the hydrothermal alteration system at Hellyer, Tasmania, as revealed by infrared reflectance spectroscopy: Journal of Geochemical Exploration, v. 108, p. 143–156.

Yarra, D.R., Peter, J.M., Harris, J., and Fueten, F., 2014, Recognition of hydrothermal alteration using airborne hyperspectral imagery and gold favourability mapping in the Hope Bay volcanic belt, Nunavut: Geological Survey of Canada, Open File 7470, 1 sheet, doi:10.4095/293727